Biotechnology and Bioengineering

WILEY

BIOTECHNOLOGY AND BIOENGINEERING

ARTICLE OPEN ACCESS

Engineering of CoA-Acylating Butyraldehyde Dehydrogenase for Enhanced 1,3-Butanediol Production in *Escherichia coli*

Seunghyun Cho[1,2] | Tayyab Islam[1,2] | Sobia Islam[1] | Junhak Lee[1,2] | Sung Won Jung[2] | Sunghoon Park[1]

[1]School of Energy and Chemical Engineering, Ulsan National Institute of Science and Technology, Ulsan, Republic of Korea | [2]R&D Center, ACTIVON Co. Ltd., Cheongju, Republic of Korea

Correspondence: Sunghoon Park (parksh@unist.ac.kr)

Received: 27 October 2025 | **Revised:** 13 March 2026 | **Accepted:** 16 March 2026

Funding: Korea Health Technology R&D Project through the Korea Health Industry Development Institute (KHIDI); Ministry of Health and Welfare, Republic of Korea, Grant/Award Number: HP23C0130

Keywords: 1,3-BDO | CoA-acylating aldehyde dehydrogenase | *E. coli* | enzyme engineering | machine-learning-guided design

ABSTRACT

Microbial production of 1,3-butanediol (1,3-BDO) offers a renewable route to this versatile C_4 chemical. However, the low performance of CoA-acylating butyraldehyde dehydrogenase (Bld), which contains a catalytic cysteine, limits efficient production in recombinant *Escherichia coli* (*E. coli*). In this study, wild-type *Clostridium saccharoperbutylacetonicum* Bld and its variant Bld* were biochemically characterized and engineered to improve conversion of 3-hydroxybutyryl-CoA (3-HB-CoA) to 3-hydroxybutyraldehyde (3-HBA). Enzyme activity was strongly reduced by the product, 3-HBA, and this reduction was largely alleviated by added cysteine. To mitigate this interference, several noncatalytic cysteine residues in Bld* were substituted individually and in combination guided by multiple sequence alignment and machine-learning-based mutational prediction. The triple mutant C151N/C189A/C353L (designated CYS31) displayed ~30% higher specific activity without altering substrate affinity or selectivity. Incorporation of CYS31 into a 1,3-BDO-producing *E. coli* strain led to a corresponding ~30% increase in titer, indicating that enhanced in vitro kinetics translated to higher in vivo 1,3-BDO production. These findings provide a more effective Bld variant for 1,3-BDO production and demonstrate that non-active-site cysteine residues can be viable engineering targets when an aldehyde intermediate is involved.

1 | Introduction

1,3-Butanediol (1,3-BDO) is a four-carbon diol used in personal-care products, food additives, and as a monomer for high-performance polyurethanes and biodegradable polyesters (Kataoka et al. 2013; T. Kim et al. 2017; Yamamoto et al. 2002). The global demand for 1,3-BDO is expected to exceed 200,000 metric tons within the next decade, yet current production relies almost exclusively on petrochemical processes involving high pressure, elevated temperature, and toxic intermediates (Global 1,3-Butylene Glycol Market n.d.). Bio-based routes using renewable feedstocks (e.g., sugars, glycerol, or CO_2) offer a sustainable alternative with reduced environmental impact and enable the production of enantiomerically pure (R)-1,3-BDO at > 98% optical purity—an advantage in pharmaceutical and specialty polymer applications (Kataoka et al. 2014; Y. Liu et al. 2021; Nemr et al. 2018). Recent advances in metabolic engineering have enabled *Escherichia coli* (*E. coli*) strains to achieve 1,3-BDO titers nearing 71.1 g L^{-1} with yields of ~0.33 g g^{-1} glucose, positioning microbial fermentation as a promising route to replace petrochemical synthesis (Islam,

Seunghyun Cho and Tayyab Islam contributed equally to this study.

Nguyen-Vo, Cho, et al. 2023). These strains typically rely on a PhaA-dependent pathway in which PhaA (acetyl-CoA acetyltransferase, EC 2.3.1.9) condenses two acetyl-CoA molecules into acetoacetyl-CoA, followed by reduction to 3-hydroxybutyryl-CoA (3-HB-CoA) via PhaB (acetoacetyl-CoA reductase, EC 1.1.1.36). A CoA-acylating aldehyde dehydrogenase then converts 3-HB-CoA to 3-hydroxybutyraldehyde (3-HBA), which is subsequently reduced to 1,3-BDO by an alcohol dehydrogenase. Among these steps, the CoA-acylating reaction represents a thermodynamic bottleneck ($\Delta G' \approx -1.5$ kJ/mol) (Beber et al. 2022) and is not efficiently catalyzed by any naturally occurring enzyme under physiological conditions.

To address this limitation, various CoA-acylating aldehyde dehydrogenases have been evaluated for their ability to support 1,3-BDO biosynthesis. These include Bld from *Clostridium saccharoperbutylacetonicum* (*C. saccharoperbutylacetonicum*; native reaction: butyryl-CoA → butyraldehyde) (Hwang et al. 2014), PduP from *Salmonella enterica* (converts propionaldehyde to propionyl-CoA) (Lan et al. 2013), and the C-terminal domain of malonyl-CoA reductase (MCR-C) from *Chloroflexus aurantiacus* (converts malonyl-CoA to malonate semialdehyde) (C. Liu et al. 2013). Of these, *Cs*Bld has shown the best in vivo performance for 1,3-BDO production in *E. coli* (Islam, Nguyen-Vo, Gaur, et al. 2023). Bld follows a ping-pong Bi-Uni-Uni-Uni mechanism: its catalytic cysteine forms a thioacyl intermediate with the acyl-CoA substrate, releasing CoA, followed by hydride transfer from NADH to form the aldehyde product (Tuck et al. 2016). Bld has also been used in synthetic pathways for 1,4-butanediol (1,4-BDO), where it converts 4-hydroxybutyryl-CoA to 4-hydroxybutyraldehyde, which is reduced to 1,4-BDO (Yim et al. 2011). Previous random mutagenesis of *Cs*Bld led to the L273T variant, which increased specific activity from ~2×10^{-3} to ~3×10^{-3} U mg^{-1} and improved 1,4-BDO titers, but the catalytic efficiency remained low (Hwang et al. 2014). Additionally, Bld is known to be oxygen-sensitive, a trait likely linked to its *Clostridial* origin. Replacing Bld with an oxygen-tolerant PduP was shown to improve *n*-butanol production under aerobic conditions (Lan et al. 2013). Aldehyde toxicity is another major challenge in microbial 1,3-BDO production. Aldehydes such as butyraldehyde and 3-HBA can react with nucleophilic amino acid residues, including cysteine and lysine, leading to reversible or irreversible enzyme inactivation (Cai et al. 2009; Grimsrud et al. 2008). Similar issues occur in glycerol-to-1,3-propanediol pathway, where 3-hydroxypropionaldehyde inactivates both glycerol dehydratase and downstream oxidoreductases. In *Klebsiella pneumoniae* DhaT, substituting cysteines moderately improved enzyme stability under aldehyde stress (Li et al. 2016).

In the present study, wild-type *Cs*Bld and a previously engineered variant Bld* (containing 11 substitutions, developed by Genomatica, Inc.) were characterized to establish baseline activity and aldehyde tolerance (Shah and Warner 2023). Aldehyde imposed product inhibition during its production but was quickly sequestered by cysteine. Distal cysteine residues in Bld* were selected as engineering targets and substitution candidates were determined through sequence alignment and machine-learning-guided mutational scoring. A library of single, double, and triple cysteine-substitution variants was constructed, and their kinetic properties and aldehyde sensitivity were evaluated in vitro, and selected variants were implemented in an engineered *E. coli* strain to assess effects on 1,3-BDO fermentation.

2 | Materials and Methods

2.1 | Materials

DNA oligonucleotides were synthesized and DNA sequencing was performed by Macrogen Co. Ltd. (Seoul, Korea). PfuX DNA polymerase was obtained from Invitrogen (Korea). Plasmid extraction and gel purification kits were from Cosmogenetech (Seoul, Korea). Restriction endonucleases, T4 DNA ligase, and other standard DNA-modifying enzymes were purchased from New England Biolabs (Ipswich, MA, USA). Yeast extract, tryptone, and agar were obtained from Difco (BD, Franklin Lakes, NJ, USA). All other chemicals (analytical grade) were from Sigma-Aldrich (St. Louis, MO, USA), unless otherwise noted.

2.2 | Plasmid Construction and Site-Directed Mutagenesis

The strains and plasmids used are listed in Table 1. The *bld* gene from *C. saccharoperbutylacetonicum* N1-4 (HMT) was codon-optimized for *E. coli* and synthesized by Macrogen (Seoul, Korea). The gene was cloned into the pQE80L vector (pQ1; Qiagen) using the BamHI and HindIII restriction sites to generate an N-terminal His_6-tagged construct (pQ1-*Cs*Bld). In parallel, a second synthetic variant carrying the 11 Genomatica mutations (Bld*) was cloned into the same pQ1 backbone to generate pQ1-Bld*. Site-directed mutagenesis of pQ1-bld* was performed with the QuikChange II kit (Agilent, Santa Clara, CA, USA) following the manufacturer's protocol. Primers were designed using the TaKaRa Bio Primer Design tool. Mutant plasmids were obtained via PCR with mutagenic primers and confirmed by Sanger DNA sequencing (Macrogen, Seoul, Korea). Multiple (double/triple) substitutions were introduced through sequential mutagenesis using validated single-mutant plasmids as templates. Plasmids were propagated in *E. coli* DH5α and isolated using a Labopass Plasmid MiniPrep kit (Cosmogenetech, Korea).

2.3 | Protein Expression and Purification

Recombinant *Cs*Bld and its variants were expressed in *E. coli* BL21(DE3) harboring pQE80L-derived plasmids. For aerobic expression, cultures were grown in 1-L Erlenmeyer flasks containing 200 mL LB medium plus kanamycin (50 μg mL^{-1}) at 37°C, 200 rpm to OD_{600} 0.6–0.8. Expression was induced with IPTG (0.5 mM) and temperature reduced to 30°C for 6 h. Cells were harvested (4000*g*, 10 min, 4°C), washed twice with 20 mM potassium phosphate (pH 7.0), and stored at −80°C. Pellets were resuspended in lysis buffer (20 mM potassium phosphate, 300 mM NaCl, 20 mM imidazole, pH 7.0) and disrupted by homogenization (GEA PandaPLUS 2000) or ultrasonication (Qsonica). Lysates were clarified (11,000*g*, 30 min, 4°C). His-tagged proteins were purified by Ni-NTA chromatography (Qiagen). After washing with lysis buffer, proteins were eluted with 20 mM potassium phosphate, 300 mM NaCl, 200 mM imidazole (pH 7.0), concentrated, and buffer-exchanged into

TABLE 1 | List of strains and plasmids used in this study.

Name	Description	Source
Strains		
E. coli K-12 MG1655	Wild-type strain	Novagen
E. coli BL21(DE3)	Protein expression host	Novagen
K22AB	*E. coli* MG1655 derivative with chromosomal integration of Ptrc-*yjgB* and replacement of *pta-ackA* with P2tac-*phaAB* (1,3-BDO production host)	Islam, Nguyen-Vo, Cho et al. (2023)
Plasmids		
pQ1	pQE80L (6 × His-tagged containing expression plasmid)	Islam, Nguyen-Vo, Cho et al. (2023)
pQ1-*Cs*Bld	pQ1 derivative encoding Bld wild type	This study
pQ1-Bld*	pQ1 derivative encoding Bld*	This study
pQ1_CYS1	pQ1 derivative encoding Bld* C33S (Cys→Ser mutant)	This study
pQ1_CYS2	pQ1 derivative encoding Bld* C151N (Cys→Asn mutant)	This study
pQ1_CYS3	pQ1 derivative encoding Bld* C151S (Cys→Ser mutant)	This study
pQ1_CYS4	pQ1 derivative encoding Bld* C189A (Cys→Ala mutant)	This study
pQ1_CYS5	pQ1 derivative encoding Bld* C189V (Cys→Val mutant)	This study
pQ1_CYS6	pQ1 derivative encoding Bld* C353L (Cys→Leu mutant)	This study
pQ1_CYS21	pQ1 derivative encoding Bld* C151N/C189A (double mutant)	This study
pQ1_CYS22	pQ1 derivative encoding Bld* C151N/C353L (double mutant)	This study
pQ1_CYS23	pQ1 derivative encoding Bld* C189A/C353L (double mutant)	This study
pQ1_CYS31	pQ1 derivative encoding Bld* C151N/C189A/C353L (triple mutant)	This study

storage buffer (20 mM potassium phosphate, 25% glycerol, pH 7.0) using 30 kDa MWCO concentrators (Sartorius), then stored at −80°C.

For anaerobic purification, cultivation was performed in sealed 250-mL serum bottles with 50 mL LB. At OD_{600} 0.6–0.8, IPTG (0.5 mM) was added and induction proceeded at 30°C as above. Lysis and chromatography were carried out in an anaerobic chamber (Coy Laboratory). All buffers were degassed and equilibrated ≥ 24 h before use.

2.4 | Enzyme Activity Assays

Protein concentrations were determined by the Bradford assay (Bio-Rad) using BSA as a standard. Purity and size were verified by SDS-PAGE. Assays were performed at 37°C, monitoring NADH oxidation at 340 nm ($\varepsilon = 6.22\ mM^{-1}\ cm^{-1}$). One unit (U) is the oxidation of 1 μmol NADH min^{-1} under assay conditions. The standard 1.0 mL assay contained 20 mM potassium phosphate (pH 7.0), 5 mM DTT, 150 μM NADH, and an appropriate amount of enzyme. After 1 min preincubation at 37°C, reactions were initiated by adding the acyl-CoA substrate, and the decrease in A_{340} was recorded for 1 min to determine the initial rate. Substrate specificity was assessed with 150 μM acetyl-CoA, propionyl-CoA, butyryl-CoA, or 3-HB-CoA.

For oxygen-sensitivity tests, enzymes purified anaerobically were assayed under air-saturated conditions (150 μM butyryl-CoA) using buffer equilibrated with air.

To examine aldehyde effects, 5 mM butyraldehyde was added during a 1-min preincubation at 37°C before substrate addition. In parallel "activity-rescue" assays, 10 mM L-cysteine (or another amino acid) was included during the same preincubation. Reactions were initiated with 150 μM butyryl-CoA (*Cs*Bld) or 150 μM 3-HB-CoA (Bld*). Where indicated, butyraldehyde was removed using a 30 kDa cutoff filter prior to assay.

2.5 | Computational Analysis

Three complementary computational approaches—GEMME (Global Epistatic Model for Mutational Effects), SCANEER (Sequence Co-evolution Analysis for Enzyme Engineering), and ESM-1b (Evolutionary Scale Modeling)—were employed to predict potentially beneficial substitutions in Bld*.

For GEMME, a family-specific multiple sequence alignment (MSA) was generated from the query sequence using HHblits (HMM–HMM iterative search) (Remmert et al. 2012) and MMseqs2 (Many-against-Many sequence search) (Steinegger and Söding 2017). The MSA was filtered to remove sequences with > 98% or < 20% identity to the query, < 80% coverage, or > 10% alignment gaps. The query sequence was placed at the top of the FASTA alignment, which served as input for GEMME. Mutational effect scores (ΔE) were then calculated, where more negative values indicate deleterious substitutions and more positive values indicate tolerated or potentially beneficial substitutions (Laine et al. 2019).

For SCANEER, the *Cs*Bld sequence was submitted to the SCANEER web server (D. Kim et al. 2022). This coevolutionary analysis produced a Sequence Co-evolution Index (SCI) score for each possible single-point mutation, reflecting the strength of local coevolutionary coupling. Mutations with higher SCI

scores were prioritized as candidates with greater evolutionary support and potential functional benefit.

For ESM-1b, a Transformer-based protein language model (Rives et al. 2021), mutational effects were predicted using the FunC_ESM pipeline. For each possible substitution, the change in sequence log-likelihood (ΔLL) was computed, with higher values indicating greater tolerance or benefit. Additionally, ESM-informed folding stability (ESM-IF) scores were used to exclude substitutions predicted to destabilize the protein structure.

By integrating results from GEMME, SCANEER, and ESM-1b, we identified candidate cysteine substitutions outside the catalytic pocket that were predicted to be well tolerated or potentially beneficial, and these were selected for experimental validation.

2.6 | 1,3-BDO Production in Flask Cultures

Engineered variants were evaluated in vivo using *E. coli* K22AB (Table 1), an *E. coli* K-12 derivative with chromosomally integrated *phaA*/*phaB* and an overexpressed NADPH-dependent 3-HBA reductase (*yjgB*). The production plasmid (pQ1 or derivatives) carrying *bld* was introduced by transformation. Flask fermentations used 250-mL Erlenmeyer flasks with 20 mL modified M9 defined medium (composition per Islam, Nguyen-Vo, Gaur, et al. 2023) with $50\,g\,L^{-1}$ glucose and $2\,g\,L^{-1}$ $(NH_4)_2SO_4$; kanamycin ($50\,\mu g\,mL^{-1}$) was included as appropriate. Seed cultures grown overnight in LB (37°C, 250 rpm) inoculated the production medium at initial OD_{600}~0.1. Cultures were incubated at 37°C, 200 rpm. IPTG (0.25 mM) was added at 0 h to induce pathway expression. Growth and products were monitored over time. All shake-flask experiments were biological triplicates; data are reported as means with ranges.

2.7 | Analytical Methods

OD_{600} was measured spectrophotometrically. Glucose, 1,3-BDO, and other extracellular metabolites were quantified by HPLC with a refractive index detector (Lee et al. 2025). Samples were filtered (0.2 μm) and analyzed on an Aminex HPX-87H column (Bio-Rad) at 65°C. The mobile phase was 2.5 mM H_2SO_4 delivered at $5.0\,mL\,min^{-1}$. Retention times were compared against authentic standards.

2.8 | Statistical Analysis

Unless stated otherwise, values are mean ± SD from three independent biological replicates ($n = 3$). Group differences were evaluated by two-way ANOVA (GraphPad Prism v8.3.0). Significance is annotated as: ns, $p \geq 0.12$; *, $p < 0.033$; **, $p < 0.002$; ***, $p < 0.001$.

3 | Results and Discussion

3.1 | Characterization of *Cs*Bld Bld*

3.1.1 | *Kinetic Properties of* CsBld *and Bld**

*Cs*Bld is a CoA-acylating aldehyde dehydrogenase from *C. saccharoperbutylacetonicum* used in engineered *E. coli* for 1,3-BDO production, but its kinetics were not fully quantified. We characterized wild-type *Cs*Bld and a mutant Bld* (harboring 11 mutations: C174S, C220V, C267A, C356T, C464I, M204R, R396H, E437P, A467V, F442N, T440H) developed by Genomatica (Shah and Warner 2023). In the 1,3-BDO pathway, both activity and selectivity are critical: excessive acetyl-CoA activity diverts flux to ethanol. Specific activities on acetyl-CoA (C2), propionyl-CoA (C3), butyryl-CoA (C4), and 3-HB-CoA were measured (Figure 1). *Cs*Bld showed the highest activity on butyryl-CoA (~$0.32\,U\,mg^{-1}$) and lowest on acetyl-CoA (~$0.1\,U\,mg^{-1}$). Bld* also favored butyryl-CoA ($6.5\,U\,mg^{-1}$) over acetyl-CoA ($0.5\,U\,mg^{-1}$) with higher absolute activities for all substrates and improved selectivity. On 3-HB-CoA, Bld* showed $2.9\,U\,mg^{-1}$, reflecting a retained native bias toward butyryl-CoA. Patent data reported ~$1.75\,U\,mg^{-1}$ on 3-HB-CoA and ~$0.25\,U\,mg^{-1}$ on acetyl-CoA (Figure S1). Assay-condition differences affect absolute values, but relative activities and selectivity were consistent. In contrast, Hwang et al. (2014) reported ~$2.3 \times 10^{-3}\,U\,mg^{-1}$ on butyryl-CoA for *Cs*Bld under different conditions.

To further evaluate the catalytic performance of Bld*, we determined its steady-state kinetic parameters with 3-HB-CoA, butyryl-CoA (B-CoA), and NADH (Table 2). With 3-HB-CoA, Bld* exhibited V_{max} $4.71 \pm 0.05\,U\,mg^{-1}$ and K_m $46.05 \pm 5.77\,\mu M$, giving k_{cat} $4.01 \pm 0.05\,s^{-1}$ and k_{cat}/K_m $8.71 \times 10^4\,M^{-1}\,s^{-1}$. For NADH, V_{max} $4.33 \pm 0.02\,U\,mg^{-1}$, K_m $34.59 \pm 2.71\,\mu M$, k_{cat} $3.69 \pm 0.02\,s^{-1}$, and k_{cat}/K_m $1.07 \times 10^5\,M^{-1}\,s^{-1}$. Butyryl-CoA was the most favorable (V_{max} $11.10 \pm 0.05\,U\,mg^{-1}$; K_m of $45.52 \pm 5.77\,\mu M$; k_{cat} $9.39 \pm 0.05\,s^{-1}$; k_{cat}/K_m $2.05 \times 10^5\,M^{-1}\,s^{-1}$), a 2.4-fold higher catalytic efficiency than with 3-HB-CoA. These data confirm enhanced activity toward 3-HB-CoA with a persistent bias toward butyryl-CoA.

3.1.2 | *Oxygen Sensitivity of Bld*

Because oxygen tolerance affects production, *Cs*Bld expressed and purified anaerobically was compared under O_2-free versus O_2-saturated buffer. Unexpectedly, anaerobically purified *Cs*Bld retained activity (~$0.32 \pm 0.03\,U\,mg^{-1}$) comparable to aerobically prepared enzyme, and decay rates were indistinguishable under both conditions (Figure 2), indicating minimal oxygen sensitivity under the conditions tested.

3.1.3 | *Aldehyde-Induced Activity Loss and Rescue by Cysteine*

The immediate product of the Bld reaction, 3-HBA, is highly reactive and can inactivate enzymes, including Bld. In DhaT, either substituting cysteine residues or adding free cysteine mitigated aldehyde-induced inactivation, consistent with cysteine residues being particularly susceptible to aldehydes (Li et al. 2016). In addition to the catalytic cysteine (C275), *Cs*Bld contains nine noncatalytic cysteine residues in the wild type and four in Bld*. To assess aldehyde effects, Bld* activity was measured in the presence of butyraldehyde (used as a surrogate for 3-HBA, which is not commercially available). Increasing butyraldehyde concentrations caused a dose-dependent decrease in activity; at 10 mM butyraldehyde, ~85% of activity was lost (Figure 3A). Notably, the toxic effect was immediate rather than time-dependent: 2 mM butyraldehyde caused an immediate ~60% loss of activity with no further decline over 60 min (Figure 3B). We next examined the influence of exogenous cysteine: Bld* was preincubated with 5 mM butyraldehyde for

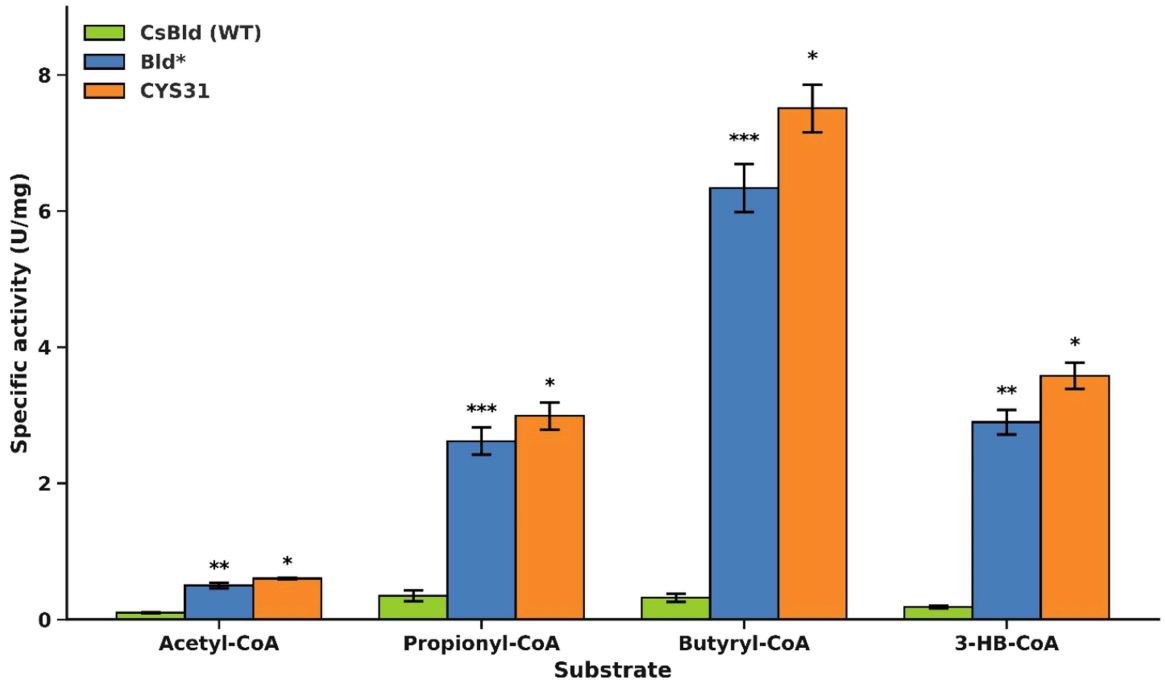

FIGURE 1 | Substrate specificity of *Cs*Bld (WT), Bld*, and CYS31. Specific activity (U mg^{-1}) toward acetyl-CoA, propionyl-CoA, butyryl-CoA, and 3-HB-CoA is shown as bars for *Cs*Bld (WT, green), Bld* (blue), and CYS31 (orange). Each substrate was added at 150 mM with NADH at the same concentration of substrate, and the activity was determined by monitoring the disappearance of NADH at 340 nm. Error Bars show mean ± SD ($n = 3$). Asterisks on Bld* bars indicate difference versus *Cs*Bld (WT); asterisks on CYS31 bars indicate difference versus Bld* ($p \leq 0.05$, *$p \leq 0.01$, **$p \leq 0.001$, ***$p \leq 0.0001$; ns not shown).

TABLE 2 | Kinetic parameters of Bld* and triple cysteine mutant CYS31.

Enzyme	Substrate	V_{max} (U/mg)	K_m (uM)	k_{cat} (s^{-1})	k_{cat}/K_m ($M^{-1} S^{-1}$)
Bld*	3-HB-CoA	4.71 ± 0.05	46.05 ± 5.77	4.01 ± 0.05	8.71×10^4
	B-CoA	11.10 ± 0.05	45.52 ± 5.77	9.39 ± 0.05	2.05×10^5
	NADH	4.33 ± 0.02	34.59 ± 2.71	3.69 ± 0.02	1.07×10^5
CYS31	3-HB-CoA	5.81 ± 0.06	44.79 ± 4.01	4.94 ± 0.05	1.10×10^5
	B-CoA	12.69 ± 0.06	40.59 ± 3.77	11.09 ± 0.05	2.74×10^5
	NADH	4.78 ± 0.02	29.92 ± 2.66	4.07 ± 0.02	1.36×10^5

1 min, followed by a 1-min incubation with cysteine at various concentrations (Figure 3C). Free cysteine substantially restored activity in a dose-dependent manner, recovering up to ~90% of the initial activity.

To further characterize the toxic effect, additional experiments were performed (Figure 4). In one, Bld* was incubated with 5 mM butyraldehyde for up to 30 min, after which the aldehyde was removed at defined time points using a cutoff filter before assaying activity. Removing the aldehyde restored > 90% of activity (Figure 4A), suggesting that aldehyde does not bind to the enzyme permanently. A second experiment tested the hypothesis that the activity reduction reflects competitive product inhibition. Initial rates were measured in the presence of 0, 1, and 5 mM butyraldehyde. Higher butyraldehyde levels produced greater inhibition and an increase in the apparent K_m for butyryl-CoA (Figure 4B). Lineweaver–Burk plots showed a nearly unchanged V_{max} with increasing product concentration, consistent with competitive inhibition by butyraldehyde (Figure 4B). The product inhibition constant was estimated as $K_i \approx 1.76$ mM. Finally, to determine whether cysteine is uniquely protective, each standard amino acid (10 mM) was added individually to assays containing 5 mM butyraldehyde (Figure 4C). Cysteine provided the strongest protection, maintaining 93% relative activity, whereas phenylalanine was a distant second (~60%). Tyrosine further reduced activity and exhibited similar inhibition even in the absence of aldehyde. Although the exact mechanism is unclear, phenylalanine likely provides nonspecific protection (e.g., hydrophobic effects), whereas tyrosine inhibits activity even without aldehyde, suggesting a direct interaction with the enzyme. Other amino acids, including lysine, showed no significant effect. Because cysteine readily reacts with aldehydes in solution without catalysis—forming hemithioacetals (favored at acidic–neutral pH) or Schiff bases/imines (favored at neutral–basic pH) Baert et al. 2015—these observations suggest that imine formation does not contribute appreciably to protection, and that cysteine-dependent hemithioacetal formation is the dominant mechanism.

Taken together, these findings indicate that butyraldehyde causes rapid and largely reversible inhibition of Bld* under the assay

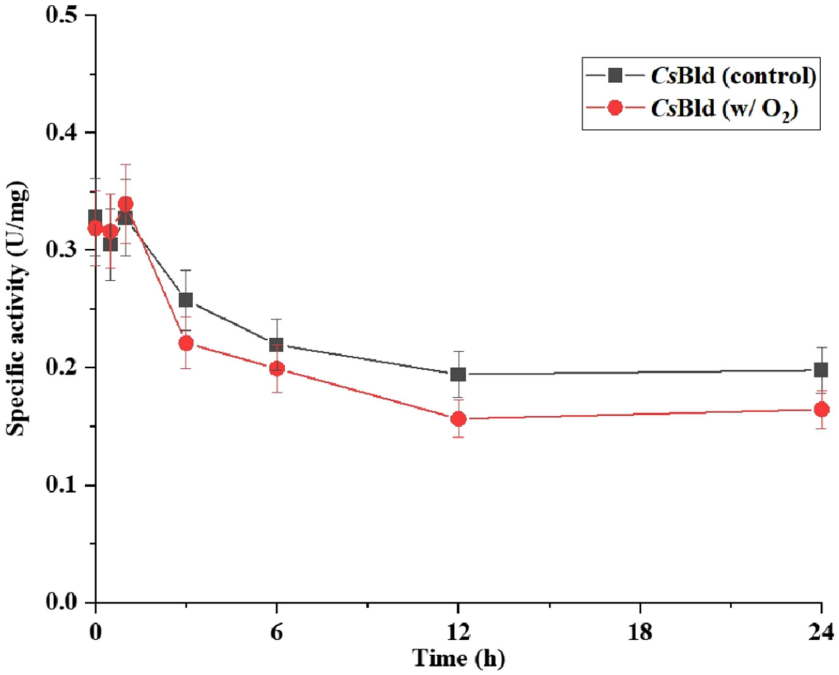

FIGURE 2 | Oxygen sensitivity of *Cs*Bld. *Cs*Bld purified under anaerobic conditions was incubated in either oxygen-free or oxygen-saturated buffer, and specific activity (U mg^{-1}) was measured at the indicated times. Error bars show mean ± SD ($n = 3$).

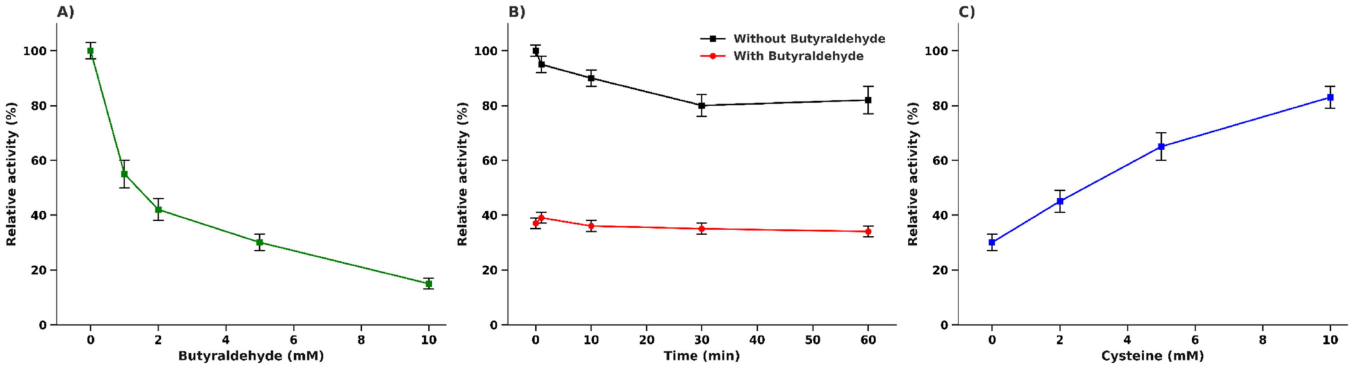

FIGURE 3 | Toxic effect of butyraldehyde on Bld*. (A) Dose-dependent loss of activity after 1 min preincubation with varying butyraldehyde concentration. (B) Time-course of enzyme activity during incubation with 2 mM butyraldehyde. (C) Recovery of activity by cysteine addition: enzyme was preincubated for 1 min with 5 mM butyraldehyde, followed by 1 min incubation with varying cysteine concentrations before assay. Error bars show mean ± SD ($n = 3$).

conditions used here, and that free cysteine alleviates this effect, likely by scavenging aldehyde in solution. Because butyraldehyde was used as a surrogate for 3-HBA, these experiments establish aldehyde sensitivity in vitro but do not quantify the extent of inhibition by 3-HBA in vivo. On this basis, we selected noncatalytic cysteine residues as engineering targets to test whether catalytic activity and/or resistance to aldehyde challenge could be improved.

3.2 | Engineering Bld* by Substituting Cysteine Residues

3.2.1 | Selection of Cysteine Mutation Targets via In Silico Analysis

To guide mutagenesis, an in silico analysis was conducted to identify promising cysteine mutations. Four complementary computational analyses (two GEMME runs using HHblits and MMseqs2, SCANEER, and ESM-1b) converged on six single-cysteine variants for Bld*: C33S, C151S, C151N, C189A, C189V, and C353L (Figure S3). In general, the tools provided complementary insights: at some sites all methods agreed on a preferred substitution, whereas at others the recommended mutations differed. For example, at position C151, all methods suggested replacing Cys with Asn. GEMME predicted no significant fitness cost for C151N ($\Delta E \approx 0$), SCANEER assigned it a high substitution confidence (~0.9), and ESM-1b indicated roughly a tenfold higher sequence likelihood for Asn over Cys. C151N was thus chosen for testing (with C151S included as a conservative alternative). C353 was another consensus site: leucine was unanimously recommended by both GEMME runs, SCANEER, and ESM-1b, making C353L an obvious choice.

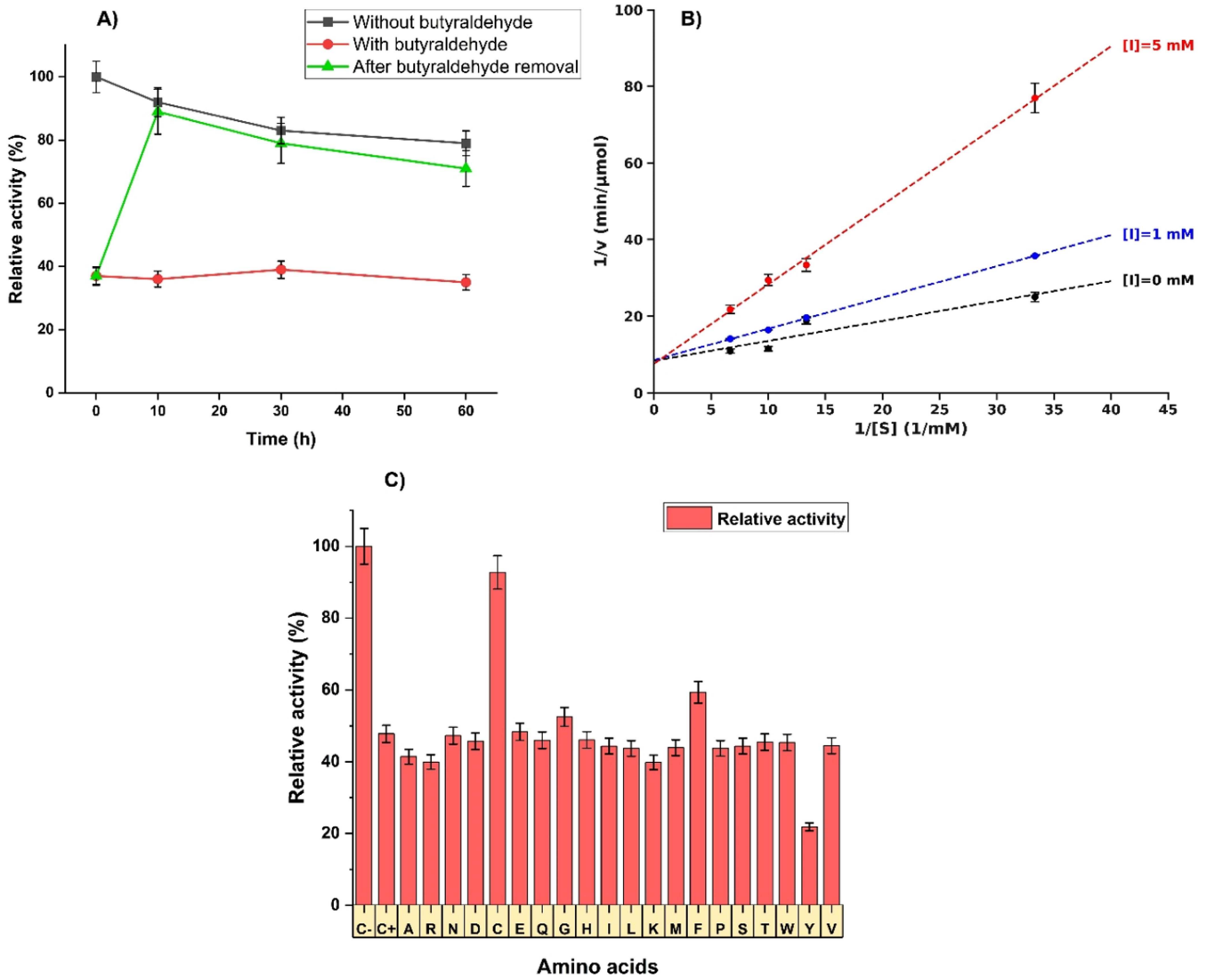

FIGURE 4 | Product inhibition of Bld* by butyraldehyde and protection by amino acids. (A) Time course of Bld* relative activity (%) under three conditions: no butyraldehyde, 5 mM butyraldehyde, and after removal of butyraldehyde with a cutoff filter at the indicated incubation times. (B) Lineweaver–Burk plots of initial rates in the presence of butyraldehyde (e.g., 0, 1, and 5 mM) to characterize product inhibition. (C) Recovery by amino acids: enzyme was preincubated for 1 min with 5 mM butyraldehyde, followed by 1 min incubation with 10 mM of the indicated amino acid before assay. Error bars show mean ± SD ($n = 3$).

Conversely, predictions for other sites were more divergent. At C33 (a poorly conserved N-terminus), no single mutation was clearly favored: GEMME's top hit varied with alignment method, and ESM-1b and SCANEER offered only marginal guidance. In the absence of a clear winner, a serine substitution (C33S) was chosen to remove the thiol with minimal structural perturbation. At C189, SCANEER did not suggest any particular substitution (indicating a weak coevolutionary signal), but GEMME ranked alanine highest (with valine second), and ESM-1b also supported both options. Thus, both C189A and C189V were included. In summary, the computational analysis yielded both consensus targets (e.g., C151N, C353L, supported by all methods) and site-specific suggestions (e.g., C33S, C189V from individual approaches), guiding our selection of cysteine substitutions in Bld*. The list of cysteine-substituted mutant enzymes is presented in Table 3.

TABLE 3 | List of cysteine substitution mutant enzymes.

Multiplicity	Name	Description
Single	CYS1	C33S
	CYS2	C151N
	CYS3	C151S
	CYS4	C189A
	CYS5	C189V
	CYS6	C353L
Double	CYS21	C151N/C189A
	CYS22	C151N/C353L
	CYS23	C189A/C353L
Triple	CYS31	C151N/C189A/C353L

3.2.2 | *Performance of Bld* Variants*

All six single-cysteine mutants were expressed and purified (Figure S4). The variants were largely soluble and yielded sufficient purified protein. These enzymes were assayed for (i) specific activity on 3-HB-CoA, (ii) stability (residual activity after aldehyde exposure), and (iii) "protectivity" (the fraction of activity preserved upon addition of cysteine). Four single mutants (C151N, C189A, C189V, C353L) retained specific activities similar to Bld*, whereas C151S showed a modest reduction and C33S exhibited a pronounced decrease (Figure 5). None of the single substitutions exceeded Bld* in activity. Stability (residual activity after aldehyde exposure) improved in C33S (~50% higher than Bld*), C151N (~38% higher), and C151S (~25% higher), but not in the other variants, suggesting that Cys33 and Cys151 are more prone to aldehyde-mediated inactivation than Cys189 or Cys353. Protectivity was similar among all single mutants (~65%–75%).

Guided by the single-mutant results, three substitutions (C151N, C189A, and C353L) were combined to form double mutants (CYS21, CYS22, and CYS23) and a triple mutant (CYS31), which were characterized using the same assays (Figure 5). Notably, CYS21 and CYS31 showed ~30% higher specific activity toward 3-HB-CoA than Bld*, whereas CYS22 and CYS23 showed no activity improvement. In contrast, stability gains under butyraldehyde challenge were modest (14%–36%) and did not parallel catalytic performance: CYS23 showed the largest stability increase, whereas CYS31 showed one of the smallest. Protectivity after butyraldehyde exposure was slightly lower in the multimutants, especially CYS22 and CYS31, than in Bld*. These results indicate that selected non-catalytic cysteine substitutions can enhance the catalytic performance of Bld, but they do not show a simple correlation between aldehyde-challenge phenotypes and the activity gains of the best-performing variants. Accordingly, the improved performance of CYS31 is most directly supported as an increase in catalytic capacity, whereas reduced susceptibility to aldehyde-mediated perturbation remains a possible but unproven contributor. Furthermore, the contrasting behaviors of CYS23 and CYS31 indicate that aldehyde-challenge stability and catalytic turnover are only partially coupled, and that the effects of distal cysteine substitutions (Figure S5) are position-dependent and nonadditive.

The best variant, CYS31, was selected for detailed kinetic characterization (Table 2). Its K_m for 3-HB-CoA was essentially unchanged (44.8 μM for CYS31 vs. 46.1 μM for Bld*), but k_{cat} increased to 4.94 s^{-1} (~25% above Bld*), yielding a ~1.26-fold higher catalytic efficiency ($k_{cat}/K_m \approx 1.10 \times 10^5$ M^{-1} s^{-1}) (Table 2.). Substrate selectivity assays showed that CYS31's activity on acetyl-CoA was 0.62 U mg^{-1}, and the activity ratios relative to acetyl-CoA were ~12.5 for butyryl-CoA and ~5.8 for 3-HB-CoA—virtually identical to Bld* (Figure 1.). Thus, CYS31 retained the substrate specificity of Bld* while achieving higher turnover on 3-HB-CoA, making it a superior biocatalyst for 1,3-BDO production.

3.3 | Application of the Improved Bld in 1,3-BDO Fermentation

In *E. coli* K22AB flask fermentations, CYS31 increased 1,3-BDO titer by ~30% compared to Bld*, with similar growth (final OD_{600}~8–9, 48 h). CYS21 and CYS22 also showed ~10%–15% higher titers (Figure 6). Titer improvements tracked with specific-activity gains, indicating the Bld-catalyzed step as an important pathway bottleneck. With higher-activity variants, glucose consumption increased, 3-HB and acetate accumulation increased, and pyruvate accumulation decreased. The greater acetate accumulation suggests increased acetyl-CoA activity alongside 3-HB-CoA activity, that is, selectivity was not improved (Figure 1). Notably, CYS23, despite similar in vitro activity to Bld*, yielded a much lower 1,3-BDO titer; acetate was

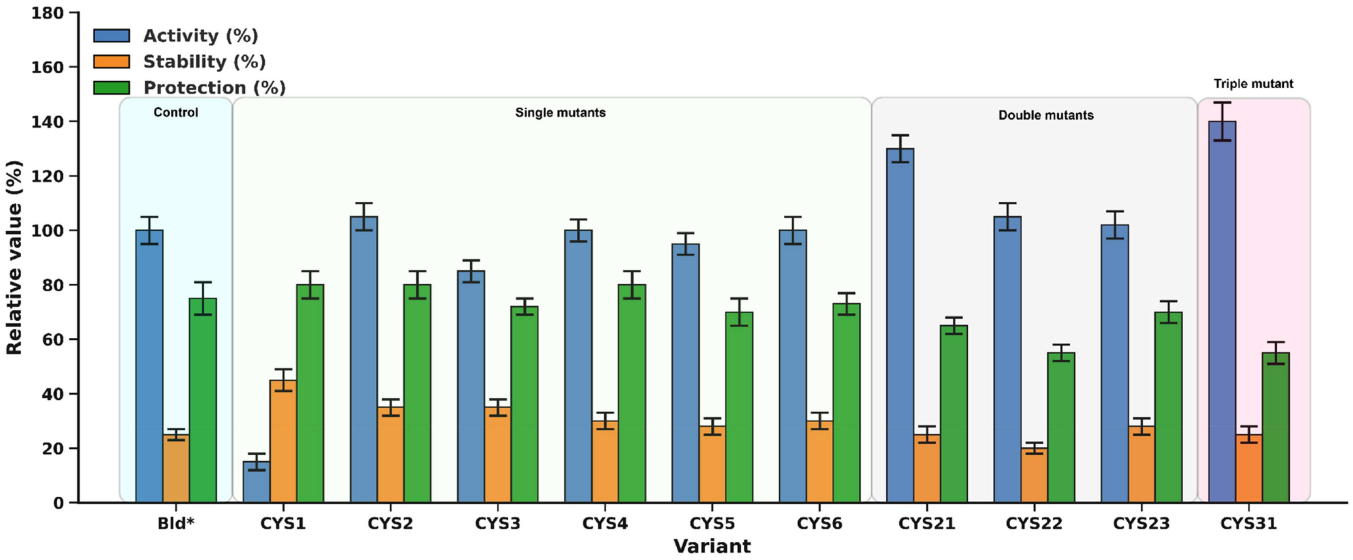

FIGURE 5 | Performance of Bld mutants, including single-, double-, and triple-site variants. Enzyme activity was assayed using 0.15 mM 3-hydroxybutyryl-CoA. For stability testing, enzymes were preincubated with 5 mM butyraldehyde for 1 min before the activity assay. To evaluate cysteine protection, enzymes were preincubated with 5 mM butyraldehyde for 1 min and then incubated with 5 mM cysteine for 1 min prior to measurement. Error bars show mean ± SD ($n = 3$).

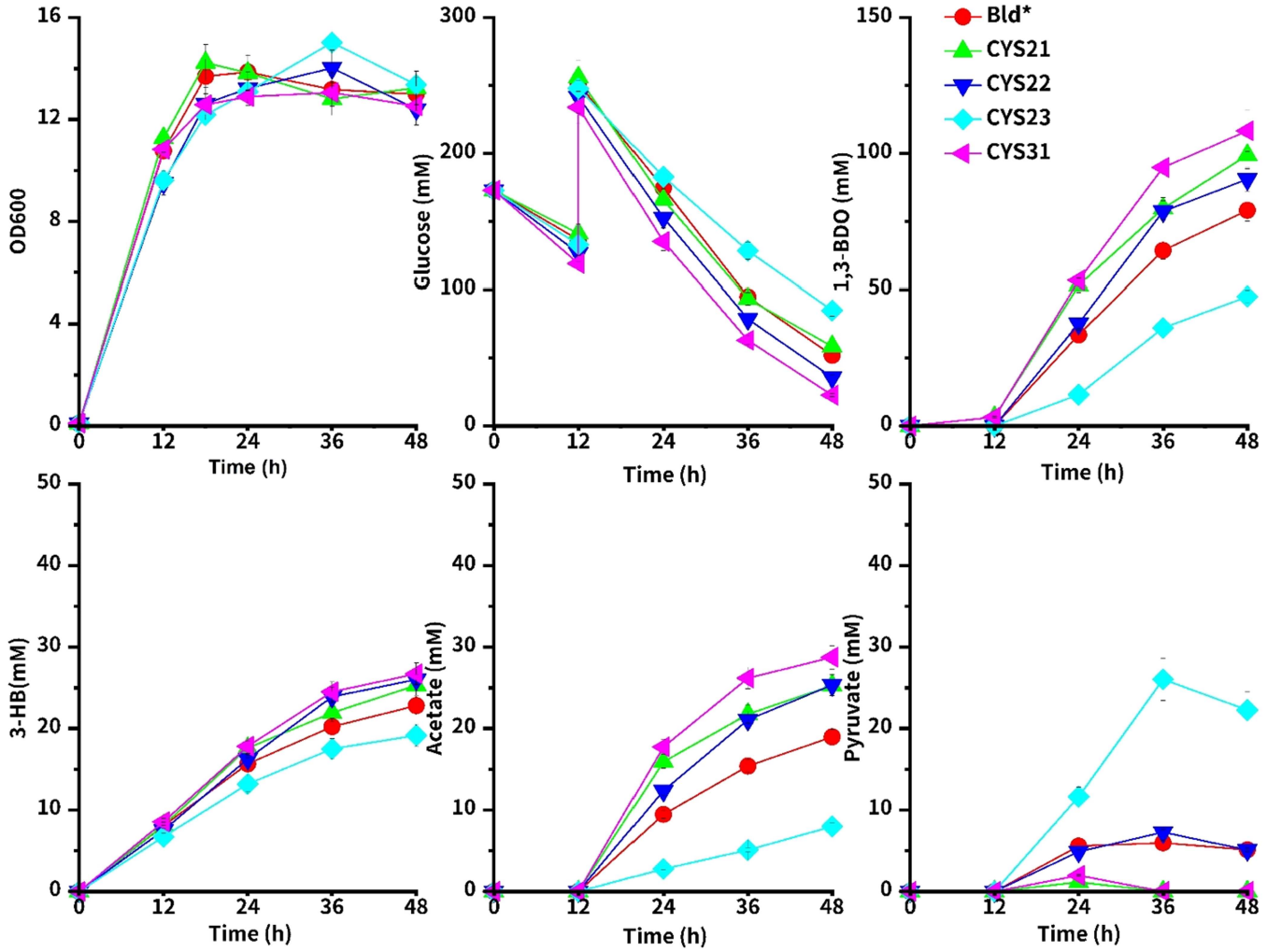

FIGURE 6 | Flask experiment for testing Bld* CYS variants in *E. coli* K22AB during 1,3-BDO production. Growth (OD_{600}), glucose consumption, and production of 1,3-BDO, 3-HB, acetate, and pyruvate were monitored over 48 h. Error bars show mean ± SD ($n = 3$).

low (~8 mM) and pyruvate high (~30 mM), indicating poor *in vivo* catalytic activity—likely lower expression. Pyruvate buildup is known to slow glucose uptake (Long et al. 2017).

This work shows how enzyme-level improvements can translate into whole-cell gains, underscoring the value of protein engineering in pathway optimization. The increase in 1,3-BDO titer observed with CYS31 closely paralleled its higher specific activity and higher k_{cat} toward 3-HB-CoA, whereas K_m and substrate selectivity remained essentially unchanged, indicating that improved catalytic turnover of the Bld step is the most direct explanation for the higher in vivo flux and product titer. Because the substituted cysteine residues are distal from the catalytic site, the beneficial effect of CYS31 is likely mediated indirectly, for example, through subtle changes in local structure or conformational dynamics that favor catalysis. Reduced susceptibility to aldehyde-mediated perturbation may also contribute, but this cannot be assessed quantitatively from the present data because butyraldehyde was used as a surrogate aldehyde and intracellular 3-HBA was not measured. If broadly applicable, similar engineering of noncatalytic cysteine residues may benefit other enzymes that process or generate aldehydes. From a practical standpoint, additional gains may face diminishing returns if CYS31 approaches catalytic potential; increased expression may then be more impactful in metabolic engineering efforts. Although an upper limit is difficult to define, the wild-type activity on butyryl-CoA (approximately double that on 3-HB-CoA) offers a rough benchmark. In CoA-acylating aldehyde dehydrogenases, hydride transfer is typically rate-limiting (Tuck et al. 2016) and common to both substrates; thus, a twofold activity increase may be realistic and beneficial by lowering the enzyme level required for a given flux.

4 | Conclusion

We engineered the CoA-acylating aldehyde dehydrogenase Bld to enhance 1,3-BDO fermentation in *E. coli*. The triple mutant CYS31 (C151N/C189A/C353L) exhibited ~30% higher specific activity than Bld* without adverse effects on affinity or selectivity, and delivered ~30% higher 1,3-BDO titers in vivo. These results highlight noncatalytic cysteine residues as impactful engineering targets in aldehyde-related reactions and underscore the value of computational guidance. Further studies to quantify intracellular 3-HBA and to improve Bld catalytic efficiency, expression, and host metabolism will be important for high-yield, industrial-scale 1,3-BDO production.

Acknowledgments

This work was supported by the Korea Health Technology R&D Project through the Korea Health Industry Development Institute (KHIDI), funded by the Ministry of Health and Welfare, Republic of Korea (Grant No. HP23C0130).

Conflicts of Interest

The authors declare no conflicts of interest.

Data Availability Statement

All the generated or analyzed data during the study are included in the manuscript.

References

Baert, J. J., J. De Clippeleer, L. De Cooman, and G. Aerts. 2015. "Exploring the Binding Behavior of Beer Staling Aldehydes in Model Systems." *Journal of the American Society of Brewing Chemists* 73, no. 1: 100–108. https://doi.org/10.1094/asbcj-2015-0109-01.

Beber, M. E., M. G. Gollub, D. Mozaffari, et al. 2022. "EQuilibrator 3.0: A Database Solution for Thermodynamic Constant Estimation." *Nucleic Acids Research* 50: D603–D609.

Cai, J., A. Bhatnagar, and W. M. Pierce. 2009. "Protein Modification by Acrolein: Formation and Stability of Cysteine Adducts." *Chemical Research in Toxicology* 22: 708–716.

Global 1,3-Butylene Glycol Market. n.d.

Grimsrud, P. A., H. Xie, T. J. Griffin, and D. A. Bernlohr. 2008. "Oxidative Stress and Covalent Modification of Protein With Bioactive Aldehydes." *Journal of Biological Chemistry* 283: 21837–21841.

Hwang, H. J., J. H. Park, J. H. Kim, et al. 2014. "Engineering of a Butyraldehyde Dehydrogenase of *Clostridium saccharoperbutylacetonicum* to Fit an Engineered 1,4-Butanediol Pathway in *Escherichia coli*." *Biotechnology and Bioengineering* 111: 1374–1384. https://doi.org/10.1002/bit.25196/abstract.

Islam, T., T. P. Nguyen-Vo, S. Cho, J. Lee, V. K. Gaur, and S. Park. 2023. "Metabolic Engineering of *Escherichia coli* for Enhanced Production of 1,3-Butanediol From Glucose." *Bioresource Technology* 389: 129814. https://doi.org/10.1016/j.biortech.2023.129814.

Islam, T., T. P. Nguyen-Vo, V. K. Gaur, J. Lee, and S. Park. 2023. "Metabolic Engineering of *Escherichia coli* for Biological Production of 1, 3-Butanediol." *Bioresource Technology* 376: 128911. https://doi.org/10.1016/j.biortech.2023.128911.

Kataoka, N., A. S. Vangnai, H. Ueda, T. Tajima, Y. Nakashimada, and J. Kato. 2014. "Enhancement of (*R*)-1,3-Butanediol Production by Engineered *Escherichia coli* Using a Bioreactor System With Strict Regulation of Overall Oxygen Transfer Coefficient and pH." *Bioscience, Biotechnology, and Biochemistry* 78: 695–700.

Kataoka, N., A. S. Vangnai, T. Tajima, Y. Nakashimada, and J. Kato. 2013. "Improvement of (*R*)-1,3-Butanediol Production by Engineered *Escherichia coli*." *Journal of Bioscience and Bioengineering* 115: 475–480.

Kim, D., M. H. Noh, M. Park, et al. 2022. "Enzyme Activity Engineering Based on Sequence Co-Evolution Analysis." *Metabolic Engineering* 74: 49–60.

Kim, T., R. Flick, J. Brunzelle, et al. 2017. "Novel Aldo-Keto Reductases for the Biocatalytic Conversion of 3- Hydroxybutanal to 1,3-Butanediol: Structural and Biochemical Studies." *Applied and Environmental Microbiology* 83, no. 7: e03172-16. https://doi.org/10.1128/AEM.03172-16.

Laine, E., Y. Karami, and A. Carbone. 2019. "GEMME: A Simple and Fast Global Epistatic Model Predicting Mutational Effects." In *Molecular Biology and Evolution*. Oxford University Press.

Lan, E. I., S. Y. Ro, and J. C. Liao. 2013. "Oxygen-Tolerant Coenzyme A-Acylating Aldehyde Dehydrogenase Facilitates Efficient Photosynthetic *n*-Butanol Biosynthesis in Cyanobacteria." *Energy & Environmental Science* 6: 2672–2681.

Lee, J., T. Islam, S. Cho, N. Arumugam, V. K. Gaur, and S. Park. 2025. "Energy Metabolism Coordination for the Byproduct-Free Biosynthesis of 1,3-Propanediol in *Escherichia coli*." *Bioresource Technology* 421: 132147. https://doi.org/10.1016/j.biortech.2025.132147.

Li, Z., S. M. Ro, B. S. Sekar, et al. 2016. "Improvement of 1,3-Propanediol Oxidoreductase (DhaT) Stability Against 3-Hydroxypropionaldehyde by Substitution of Cysteine Residues." *Biotechnology and Bioprocess Engineering* 21: 695–703.

Liu, C., Q. Wang, M. Xian, Y. Ding, and G. Zhao. 2013. "Dissection of Malonyl-Coenzyme A Reductase of *Chloroflexus aurantiacus* Results in Enzyme Activity Improvement." *PLoS One* 8: e75554.

Liu, Y., X. Cen, D. Liu, and Z. Chen. 2021. "Metabolic Engineering of *Escherichia coli* for High-Yield Production of (*R*)-1,3-Butanediol." *ACS Synthetic Biology* 10: 1946–1955.

Long, C. P., J. Au, N. R. Sandoval, N. A. Gebreselassie, and M. R. Antoniewicz. 2017. "Enzyme I Facilitates Reverse Flux From Pyruvate to Phosphoenolpyruvate in *Escherichia coli*." *Nature Communications* 8, no. 1. https://doi.org/10.1038/ncomms14316.

Nemr, K., J. E. N. Müller, J. C. Joo, et al. 2018. "Engineering a Short, Aldolase-Based Pathway for (*R*)-1,3-Butanediol Production in *Escherichia coli*." *Metabolic Engineering* 48: 13–24.

Remmert, M., A. Biegert, A. Hauser, and J. Söding. 2012. "HHblits: Lightning-Fast Iterative Protein Sequence Searching by HMM-HMM Alignment." *Nature Methods* 9: 173–175.

Rives, A., J. Meier, T. Sercu, et al. 2021. "Biological Structure and Function Emerge From Scaling Unsupervised Learning to 250 Million Protein Sequences." *Proceedings of the National Academy of Sciences* 118, no. 15: e2016239118. https://www.pnas.org.

Shah, A., and J. Warner. 2023. *Aldehyde Dehydrogenase Variants and Methods of Using Same*. US11634692.

Steinegger, M., and J. Söding. 2017. "MMseqs2 Enables Sensitive Protein Sequence Searching for the Analysis of Massive Data Sets." In *Nature Biotechnology*. Nature Publishing Group.

Tuck, L. R., K. Altenbach, T. F. Ang, et al. 2016. "Insight Into Coenzyme A Cofactor Binding and the Mechanism of Acyl-Transfer in an Acylating Aldehyde Dehydrogenase From *Clostridium phytofermentans*." *Scientific Reports* 6: 22108.

Yamamoto, H., A. Matsuyama, and Y. Kobayashi. 2002. "Synthesis of (*R*)-1,3-Butanediol by Enantioselective Oxidation Using Whole Recombinant *Escherichia coli* Cells Expressing (S)-Specific Secondary Alcohol Dehydrogenase." *Bioscience, Biotechnology, and Biochemistry* 66: 925–927.

Yim, H., R. Haselbeck, W. Niu, et al. 2011. "Metabolic Engineering of *Escherichia coli* for Direct Production of 1,4-Butanediol." *Nature Chemical Biology* 7: 445–452.

Supporting Information

Additional supporting information can be found online in the Supporting Information section.
Supplementary Figure S1: (A) Specific activity of the wild-type enzyme and variants derived from CsBld. **Supplementary Figure S2:** Multiple sequence alignment of CsBld (Q7X4B7), CbBld (Q9X681), and the engineered variant Bld*. **Supplementary Figure S3:** Computational analysis of cysteine mutagenesis in Bld*. **Supplementary Figure S4:** SDS–PAGE analysis of enzyme purification. **Supplementary Figure S5:** Locations of cysteine residues substituted in the Bld* variant.